Scaled model experiment of long-range across-slope pulse propagation in a penetrable wedge

Alexios Korakas and Frédéric Sturm
LMFA UMR CNRS 5509, Ecole Centrale de Lyon, 36 avenue Guy de Collongue, 69134 Ecully Cedex, France
alexis.korakas@ec-lyon.fr, frederic.sturm@ec-lyon.fr

Jean-Pierre Sessarego and Didier Ferrand
LMA UPR CNRS 7051, 31 chemin Joseph Aiguier, 13402 Marseille, France
sessarego@lma.cnrs-mrs.fr, ferrand@lma.cnrs-mrs.fr

Abstract: In this paper, laboratory scale measurements of long-range across-slope propagation of broadband pulses in a shallow-water wedge-shaped environment with a sandy bottom are reported. The scaled model was designed to study the three-dimensional (3D) acoustic field in the presence of only a few propagating modes. The recorded time series exhibit prominent 3D effects such as mode shadow zones and multiple mode arrivals. Inspection of the spectral content of the time signals gives evidence of intra-mode interference and frequency dependence of the mode cut-off range in the across-slope direction.

PACS numbers: 43.30.Zk, 43.30.Bp, 43.30.Gv [JL]
Date Received: December 2, 2008 **Date Accepted:** April 22, 2009

1. Introduction

It is well known that in realistic three-dimensional (3D) oceanic environments, the acoustic propagation may be affected by the horizontal refraction of the sound energy. The effects of horizontal refraction, commonly referred to as 3D effects, require fully 3D modeling to be accounted for. During the past decades, the 3D wedge-shaped oceanic waveguide has received considerable attention as it approximates realistic oceanic environments such as the continental slope. In this specific environment, the 3D effects are perceived in the across-slope direction rather than in the up-/down-slope direction. Most of the modeling efforts to identify and quantify the 3D effects for the wedge problem focused on single-frequency considerations (see Ref. 1 for a detailed bibliography). Although computationally more intensive, the broadband approach provides a more complete and straightforward picture for the analysis of 3D effects. The broadband modeling of the 3D wedge was implemented using either a ray method[2] or a parabolic equation (PE) approach,[3] both considering a penetrable bottom. On the other hand, a number of laboratory scale experiments were conducted to investigate acoustic propagation in this particular environment and compare theoretical predictions to experimental data. Part of these experimental studies intended to examine up-slope[4] or down-slope[5] propagation alone, while others also investigated the 3D aspect of across-slope propagation.[6,7] More specifically, Ref. 6 reported results of continuous wave (cw) and pulse propagation over a perfectly reflecting bottom, and Ref. 7 investigated cw propagation considering a penetrable bottom. Both concluded to good agreement with single-frequency numerical predictions.

In this paper, we present laboratory scale measurements of long-range across-slope propagation of broadband pulses in a shallow-water wedge-shaped waveguide with a penetrable bottom. This work is part of a research program for the investigation of long-range propagation of acoustic waves in well-defined oceanic waveguides. The campaign reported here was preceded by a calibration phase that was achieved in a Pekeris-like configuration.[8] The bathymetry was subsequently modified to simulate a wedge-shaped oceanic waveguide. Preliminary tests of across-slope pulse propagation exhibited evident 3D effects and comparisons of the experimental results with numerical predictions by a fully 3D PE based code turned out to be very

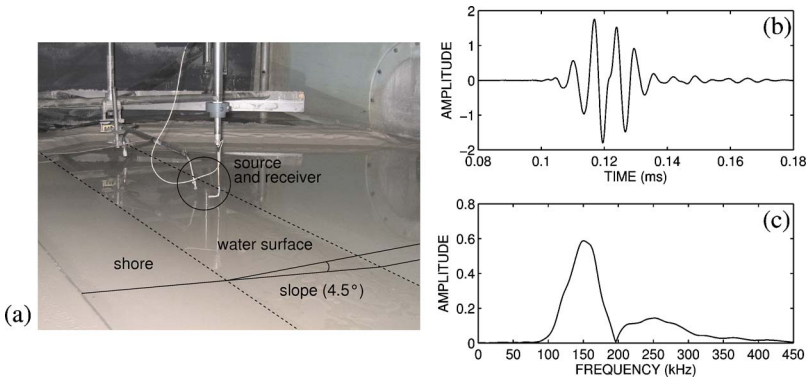

Fig. 1. (Color online) (a) Model experiment of the wedge-shaped oceanic waveguide (with a slope of approximately 4.5°), (b) source signal recorded in free-field, and (c) its frequency spectrum.

encouraging.[9] In this work, additional series of experimental measurements in the wedge-like environment are reported. The signals were recorded on a fine spatial grid within a vertical plane along the across-slope direction. To facilitate the analysis of the 3D effects, the experiment was designed to keep the number of propagating modes in the waveguide relatively low. The recorded time series exhibit strong 3D effects that are identical to those described in the literature.[1–3,6,7,10,11] The frequency dependence of the mode cut-off range is illustrated by inspecting the spectral content of the time signals recorded at several ranges. The data sets obtained during this measurement campaign are intended for 3D model-comparisons. In Sec. 2, a short description of the experimental set-up is given. Then, the experimental results are interpreted according to theoretical predictions. Results and future directions are discussed in Sec. 4.

2. Experimental set-up

The measurement campaign was conducted at the indoor tank facilities of the LMA-CNRS laboratory in Marseille (France). The shallow-water tank is 10-m-long and 3-m-wide, thus allowing for long-range propagation measurements. It consists of a thin layer of water over a thick layer of calibrated sand simulating a bottom half-space. The grain size of the sand is considerably smaller than a wavelength at the operational frequencies. The objective was to set-up a wedge-like configuration and measure the across-slope propagation up to long ranges. For this reason the sandy bottom was tilted with the wedge apex aligned along the longer side of the tank, and was made as flat as possible, see Fig. 1(a). The slope angle was approximately 4.5°. The source and receiver were cylindrical piezoelectric transducers both with diameters of approximately 6.0 mm. They can be seen in Fig. 1(a). The source could be positioned at any depth and the receiver was allowed to move in the three directions. For a detailed description of the experimental facilities and procedures, we refer to Refs. 8 and 9.

3. Experimental results

Prior to the measurements in the shallow-water tank, the source signal was analyzed in a deep-water tank. The signal recorded at a distance of 68 mm from the source appeared well separated in time from its surface echo. It is shown in Fig. 1(b). It is a 5-cycle Gaussian pulse of 40-μs duration with a weak tail of about the same duration most likely due to the mechanical response of the transducer. Its frequency spectrum presents a main lobe, carrying most of the acoustical energy, centered at approximately 150 kHz with a 100-kHz bandwidth, and a secondary lobe with a maximum at 250 kHz. The water depth at the source was 48 mm (± 1 mm) and the water sound speed was 1488.9 m/s (± 0.3 m/s). The bottom compressional wave speed and attenuation were 1700 m/s (± 50 m/s) and 0.5 dB/wavelength (± 0.1 dB/wavelength) respectively, and the bottom density was 1.99 g/cm^3 (± 0.01 g/cm^3). A preliminary simulation with a two-dimensional normal mode code showed the existence of four trapped modes at 150 kHz corre-

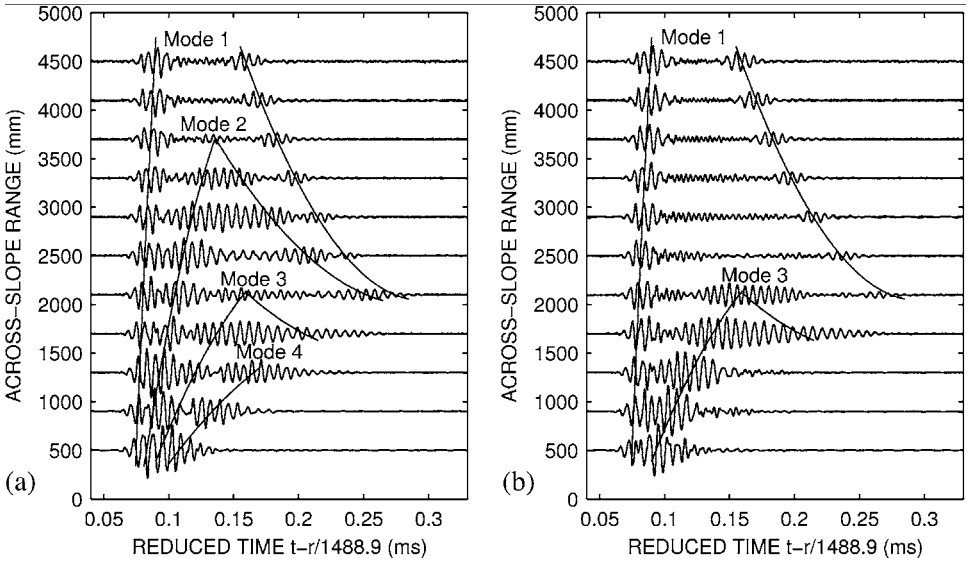

Fig. 2. Stacked time series vs source/receiver range along the across-slope direction. The source depth is 10 mm and the receiver depth is (a) 20 mm where no modal nulls occur and (b) 26 mm where modes 2 and 4 almost vanish. The lines superimposed on both panels indicate the evolution of the mode arrivals with range.

sponding to the center frequency of the main lobe. During the measurements the source was fixed at a depth of 10 mm (±0.5 mm). The received signal was recorded along the across-slope direction at several source/receiver distances from 100 to 5000 mm (±2 mm) with increments of 100 mm, and, at each range step, it was recorded at depths between 4 and 45 mm (±0.5 mm) with a depth increment of 1 mm. The results are presented in Figs. 2, 3(a), and 3(b).

Figure 2 shows two range stacks of the time signals recorded in the across-slope direction at receiver depths of 20 mm [Fig. 2(a)] and 26 mm [Fig. 2(b)]. Note that the experimental data were scaled appropriately to compensate for cylindrical spreading. The curved lines superimposed on the time series were drawn approximately to indicate the modal separation of the initial pulse with range. Four distinct modes are overall identified by simple inspection of the nulls in the depth stacks at each specific range (except at short ranges). For instance, the upper panels of Fig. 3 show the depth stacks at two distinct ranges: one at 2100 mm with modes 1–3 identified [Fig. 3(a)], and one at 2900 mm with only modes 1 and 2 identified [Fig. 3(b)]. Beyond the range of 1000 mm (i.e., ≈100 wavelengths) the time series in Fig. 2 exhibit evident 3D effects. Each mode in Fig. 2(a), with the exception of mode 4, presents two distinguishable time arrivals at some range. The relative time delay between these two arrivals decreases with increasing range. At a certain range, the two arrivals merge together and form what appears to be a more dispersed modal wave packet. Farther in range across-slope, the "merged" modal wave packet shortens and weakens, before entering into a shadow zone. Note that this shadow zone occurs at shorter ranges for higher modes. As can be seen in Fig. 2(b), modes 2 and 4 almost vanish at a receiver depth of 26 mm, and modes 1 and 3 are now separate even at short ranges. Note lastly that the noise-like signals observed between the two arrivals of mode 1 beyond the range of 4000 mm in Fig. 2(a), mainly originate from the secondary lobe of the spectrum displayed in Fig. 1(c). However, their low signal-to-noise ratio did not permit us to perform a more detailed analysis.

Mode shadow zones and multiple mode arrivals over a sloping bottom can be straightforwardly explained by means of ray/mode analogies.[10,11] Let us first consider the problem at a fixed frequency. A given mode propagates as a ray along hyperbolic paths in the horizontal plane, being gradually refracted toward regions of deeper water. As shown in Fig. 3(c), a modal-ray launched obliquely toward the wedge apex travels up-slope, and then turns back down-slope

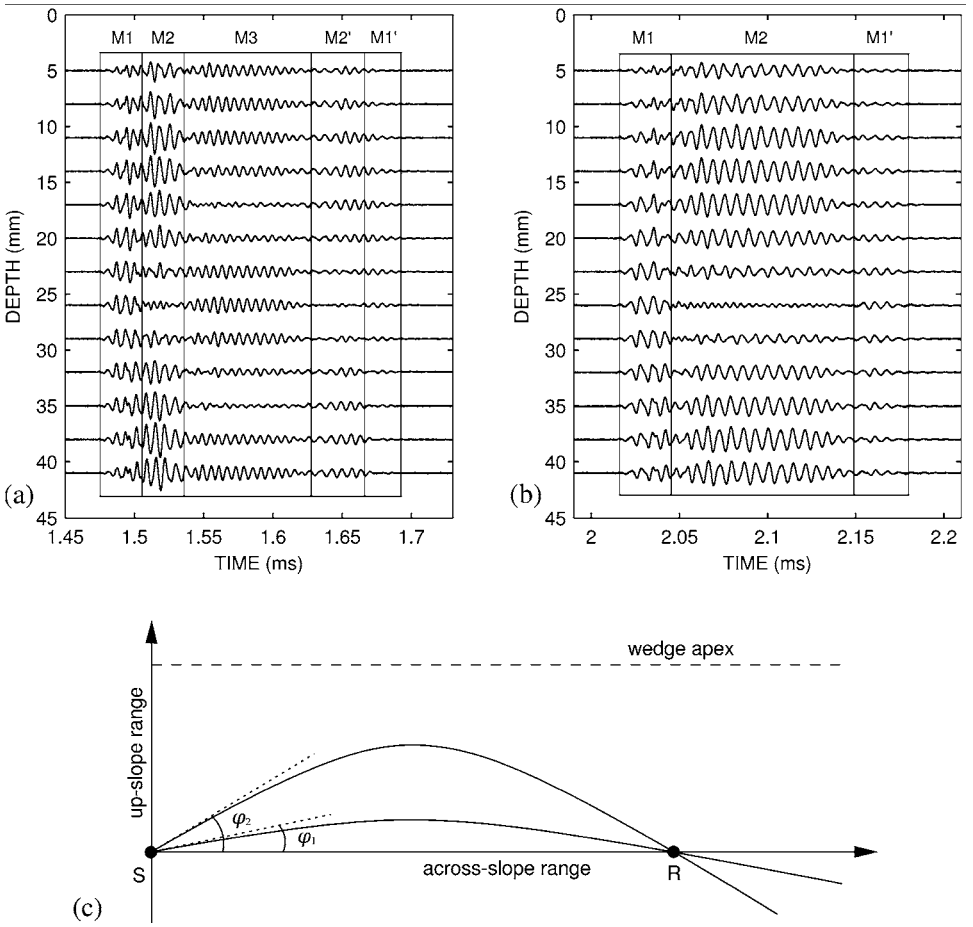

Fig. 3. Stacked time series vs receiver depth: (a) the receiver is at an across-slope range of 2100 mm. From left to right in (a), we identify the first arrival of modes 1 (M1) and 2 (M2), two merged arrivals of mode 3 (M3), a second arrival of mode 2 (M2′), and a very weak second arrival of mode 1 (M1′). (b) The receiver is at an across-slope range of 2900 mm. From left to right in (b), we identify a first arrival of mode 1 (M1), two merged arrivals of mode 2 (M2), and a now more pronounced second arrival of mode 1 (M1′). (c) Horizontal projection of modal-ray paths in the wedge environment. The receiver R positioned across-slope may see two distinct arrivals of the same mode, originating from modal-rays launched from the source S at different angles $\varphi_2 > \varphi_1$.

to intersect the across-slope direction at some range. As the horizontal launch angle, φ, with respect to the across-slope direction increases, the curvature of the modal-ray path increases, and the intersection with the across-slope occurs at shorter ranges. As a result, a receiver R positioned across-slope may see two time arrivals of the same mode: a first mode arrival launched at a low angle φ_1 and a second mode arrival launched at a higher angle φ_2. The modal-ray corresponding to the second arrival passes through regions of shallower depths leaking more energy into the bottom. Hence, the second arrival is weaker than the first arrival. Beyond a critical launch angle the modal-ray passes through its mode cut-off depth, the respective mode being thus transmitted into the bottom.[11] This explains why multiple arrivals of modes 1–3 are not observed at short ranges in Fig. 2(a), while mode 4 does not exhibit any second arrival. On the other hand, the modal-ray is subjected to less bottom loss when launched at a lower angle. This, in turn, explains the amplitude increase in the second arrival of mode 1 with increasing range, in Fig. 2. Continuing this analysis, a high-angle mode arrival has traveled a longer distance than a low-angle mode arrival. As we move out in range across-slope, the difference in the

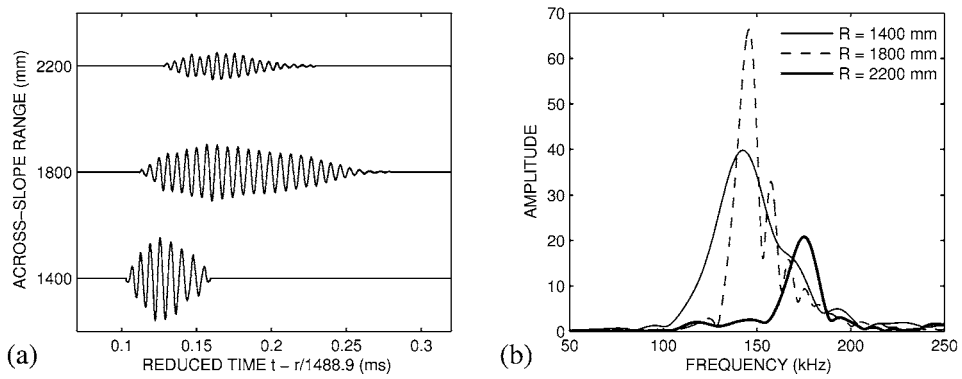

Fig. 4. (a) Mode-3 wave packet at three different ranges: at the range of 1400 mm, one arrival occurs, while two merged arrivals are observed at 1800 and 2200 mm. (b) Spectra of mode 3 at ranges of 1400, 1800, and 2200 mm, giving evidence of the range dependence of the mode cut-on frequency.

distance traveled by each of the two arrivals decreases. Accordingly, the relative time delay between these two arrivals decreases. Furthermore, as mode energy is continuously refracted down-slope, each mode reaches eventually a cut-off range beyond which its shadow zone extends. Since higher-order modes have larger incident angles to the bottom, they are refracted more abruptly. It turns out that, with increasing mode number, mode cut-off occurs at a shorter range. The experimental results presented in Fig. 2 are in complete qualitative agreement with these observations.

Let us now address the frequency dependence of the sound field. Several publications showed that the cut-off range of a given mode is shifted out in range with increasing frequency.[2,6,7,10,11] We thus expect the lower frequency part of the energy of each mode to be progressively removed due to down-slope refraction as we move out across-slope. As a consequence, the extinction of a given modal wave packet is expected to take place in an extended region along the across-slope direction. Figure 4 shows the wave packets associated to mode 3 [Fig. 4(a)] and their frequency spectra [Fig. 4(b)] at three distinct ranges: 1400, 1800, and 2200 mm. Note that mode 3 was extracted from the results of Fig. 2(b) and weighted with a Hanning window to smooth the edges. The frequency spectra were obtained as Fourier transforms of the windowed signals. As observed in Fig. 4(a), at the range of 1400 mm one single arrival of mode 3 occurs, whereas two merged arrivals are observed at the subsequent ranges (1800 and 2200 mm). In Fig. 4(b), the range dependence of the cut-on frequency of mode 3 is evident. More precisely, at the range of 1400 mm, no cut-off has taken place yet, and the cut-on frequency of the mode is approximately 100 kHz. Then, at the range of 1800 mm its cut-on frequency has moved to approximately 130 kHz, leaving the part of the spectrum up to that frequency in the shadow zone. Finally, at the range of 2200 mm, the cut-on frequency is approximately 160 kHz. Moreover, by comparing the spectra at 1400 and 1800 mm in Fig. 4(b), the peak amplitude is seen to almost double, giving evidence of an additional arrival of mode 3 at 1800 mm. Note also the interference patterns present in the spectrum of mode 3 at 1800 mm [dashed curve in Fig. 4(b)]. They are attributed to an effect known in the literature as intra-mode interference,[11] i.e., the mutual interference between arrivals of the same mode occurring at different times. These interference patterns depend on the relative time delay of the two arrivals. At the range of 2200 mm, these arrivals are almost simultaneous and intra-mode interference is weakly observed [bold curve in Fig. 4(b)]. Similar observations hold for other modes (results not shown here).

4. Conclusion and discussion

Results of scaled laboratory experiments of long-range across-slope propagation of broadband pulses in a 3D penetrable wedge were reported. The number of modes contributing to the acous-

tic field was intentionally kept relatively low. Prominent 3D effects such as modal shadow zones and multiple mode arrivals were observed experimentally in agreement with theoretical predictions. Furthermore, intra-mode interference and the frequency dependence of mode cut-off range (or, equivalently, the range dependence of mode cut-on frequency) were put in evidence by examining the spectral content of mode 3 along the across-slope direction.

To conclude, we note that, in contrast with at-sea experiments, high quality data can be collected in laboratory conditions that are suitable for comparisons with numerical propagation models. In this perspective, the experiment was designed to finely sample the sound field in the across-slope direction in both range and depth. The recorded time series can now be appropriately transformed to provide frequency-domain data at several frequencies, e.g., to obtain transmission loss vs across-slope range or depth curves. The data sets obtained during the measurement campaign turn out to be promising for future use as a real-data benchmark for 3D model-comparison. Current work focuses onto detailed comparisons of the experimental data with a fully 3D PE code.

References and links

[1]A. Tolstoy, "3-D propagation issues and models," J. Comput. Acoust. **4**, 243–271 (1996).
[2]E. K. Westwood, "Broadband modeling of the three-dimensional penetrable wedge," J. Acoust. Soc. Am. **92**, 2212–2222 (1992).
[3]F. Sturm, "Numerical study of broadband sound pulse propagation in three-dimensional oceanic waveguides," J. Acoust. Soc. Am. **117**, 1058–1079 (2005).
[4]H. Hobaek and E. K. Westwood, "Measurements of upslope wave-front curvature in a sand-bottom wedge," J. Acoust. Soc. Am. **84**, 1787–1790 (1988).
[5]C. T. Tindle, H. Hobaek, and T. G. Muir, "Normal mode filtering for downslope propagation in a shallow water wedge," J. Acoust. Soc. Am. **81**, 287–294 (1987).
[6]S. A. L. Glegg and J. R. Yoon, "Experimental measurements of three-dimensional propagation in a wedge-shaped ocean with pressure-release boundary conditions," J. Acoust. Soc. Am. **87**, 101–105 (1990).
[7]S. A. L. Glegg, G. B. Deane, and I. G. House, "Comparison between theory and model scale measurements of three-dimensional sound propagation in a shear supporting penetrable wedge," J. Acoust. Soc. Am. **94**, 2334–2342 (1993).
[8]P. Papadakis, M. Taroudakis, F. Sturm, P. Sanchez, and J.-P. Sessarego, "Scaled laboratory experiments of shallow water acoustic propagation: Calibration phase," Acta. Acust. Acust. **94**, 676–684 (2008).
[9]F. Sturm, J.-P. Sessarego, and D. Ferrand, "Laboratory scale measurements of across-slope sound propagation over a wedge-shaped bottom," in Proceedings of the Second International Conference & Exhibition on Underwater Acoustic Measurements, Greece, 2007, pp. 1151–1156.
[10]C. H. Harrison, "Acoustic shadow zones in the horizontal plane," J. Acoust. Soc. Am. **65**, 56–61 (1979).
[11]M. J. Buckingham, "Theory of three-dimensional acoustic propagation in a wedgelike ocean with a penetrable bottom," J. Acoust. Soc. Am. **82**, 198–210 (1987).